

Simulating the growth response of aspen to elevated ozone: a mechanistic approach to scaling a leaf-level model of ozone effects on photosynthesis to a complex canopy architecture☆

M.J. Martin^{a,*}, G.E. Host^a, K.E. Lenz^b, J.G. Isebrands^c

^aNatural Resources Research Institute, University of Minnesota, 5013 Miller Trunk Highway, Duluth, MN 55811, USA

^bDepartment of Mathematics and Statistics, University of Minnesota, University Drive, Duluth, MN 55812, USA

^cUSDA Forestry Service, North Central Forest Experiment Station, Forestry Sciences Laboratory, 5985 Highway K, Rhinelander, WI 54501, USA

Received 1 October 2000; accepted 17 July 2001

“Capsule”: *A process model is described that predicts the relative effects of ozone on the growth of an ozone-sensitive aspen clone.*

Abstract

Predicting ozone-induced reduction of carbon sequestration of forests under elevated tropospheric ozone concentrations requires robust mechanistic leaf-level models, scaled up to whole tree and stand level. As ozone effects depend on genotype, the ability to predict these effects on forest carbon cycling via competitive response between genotypes will also be required. This study tests a process-based model that predicts the relative effects of ozone on the photosynthetic rate and growth of an ozone-sensitive aspen clone, as a first step in simulating the competitive response of genotypes to atmospheric and climate change. The resulting composite model simulated the relative above ground growth response of ozone-sensitive aspen clone 259 exposed to square wave variation in ozone concentration. This included a greater effect on stem diameter than on stem height, earlier leaf abscission, and reduced stem and leaf dry matter production at the end of the growing season. Further development of the model to reduce predictive uncertainty is discussed. © 2001 Published by Elsevier Science Ltd. All rights reserved.

Keywords: Ozone; Photosynthesis; Aspen; Tree growth; Global change; Modelling; ECOPHYS

1. Introduction

Atmospheric and climate changes are affecting the productivity of North American forests (Melillo et al., 1996; McLaughlin and Percy, 1999; Kirschbaum, 2000), and young to middle-aged forests are playing an increasingly important role in long-term carbon sequestration (Melillo et al., 1996). However, due to the complexity and relatively large spatial and temporal scale of forest ecosystems and ecosystem processes, predictions of forest response to future environmental change will

require modelling techniques based on the mechanisms that underlie tree growth and dry matter production. The most fundamental process of vegetative growth is photosynthesis, which determines the maximum potential rate of carbon uptake by vegetation (Long, 1994). The photosynthetic response to global environmental changes such as increased concentrations of ozone and carbon dioxide depend on genotype. Therefore forest models need to be able to predict competitive interactions within a forest stand, to determine how changes in the composition and abundance of genotypes might alter potential carbon sequestration (Constable and Friend, 2000).

Atmospheric concentrations of CO₂, the substrate of photosynthesis, have increased from pre-industrial levels of approximately 280 μmol mol⁻¹ to current values of more than 360 μmol mol⁻¹, and continue to rise at an estimated rate of 1.5–2 μmol mol⁻¹ per year (IPCC, 1996). A metaanalysis, based on experimental

☆ This paper was presented at the IUFRO 19th International Meeting for Specialists in Air Pollution Effects on Forest Ecosystems, held in Houghton, Michigan, 28–31 May 2000.

* Corresponding author at: Department of Biological Sciences, University of Essex, John Tabor Laboratories, Wivenhoe Park, Colchester, Essex CO4 3SQ, UK.

E-mail address: marionmartin@compuserve.com (M.J. Martin).

results on young trees, indicates tree growth rates may be expected to increase under elevated CO₂ (Norby et al., 1999). However, the potential increase in forest biomass production and associated carbon dioxide sequestration resulting from increased growth rates may be moderated by the interacting effects of other changing conditions, such as temperature (Long, 1991), soil nutrient deficiency (Stitt and Krapp, 1999) and increasing concentrations of phytotoxic ozone (Long, 1994; McKee et al., 1995; Schmieden and Wild, 1995).

Tropospheric concentrations of ozone have risen at an estimated annual rate of 1% in the northern hemisphere for the last few decades (PORG, 1993). Increasing ozone concentrations threaten to reduce potential forest dry matter production as background concentrations are already close to harmful levels (PORG, 1993) and ozone, formed by a complex suite of reactions between hydrocarbons and nitrogen oxides in sunlight, may be transported over long distances to relatively pristine environments (Chameides et al., 1994).

Although the phytotoxic effects of highly reactive ozone have been reported for several decades (Heath, 1987; Krupa and Manning, 1988), the complex suite of reactions within the leaf that convert ozone into reactive oxygen intermediaries (ROI), together with the resultant production of a variety of possible protective scavenging mechanisms, has made it difficult to establish the biochemical mechanisms of ozone damage (Heath, 1994; Pell et al., 1994, 1999). Although concentrations of ambient ozone close to background levels of 20–30 nmol m⁻² s⁻¹ have no significant effects on photosynthesis, concentrations of 60 nmol m⁻² s⁻¹ and above may impair photosynthetic functioning within the mesophyll (McKee et al., 1995; Farage, 1996). The primary effect of chronic and acute ozone exposure on photosynthesis in wheat is a reduction in the maximum capacity of carboxylation (V_{cmax}), thereby inducing stomatal closure via an increase in intercellular [CO₂] (Farage et al., 1991; McKee et al., 1995; Farage and Long, 1999). Indeed, stomatal closure observed in wheat under the acute ozone experiments of Farage et al. (1991) could be explained solely by the decrease in V_{cmax} , via the predicted change in intercellular CO₂ concentration (Martin et al., 2000). Ozone also reduces the photosynthetic capacity and growth of the ozone-sensitive clone 259 of trembling aspen (*Populus tremuloides*) (Coleman et al., 1995a; Kull et al., 1996; Karnosky et al., 1996, 1999). Other symptoms of ozone damage reported for aspen include black bifacial necrosis, and upper leaf surface black or red stipple, a loss of chlorophyll, accelerated leaf senescence associated with earlier leaf abscission, changes in carbon allocation patterns and reduction in productivity and growth (Coleman et al., 1995b; Kull et al., 1996; Karnosky et al., 1999; Yun and Laurence, 1999). By scaling a leaf-level model to the whole tree, it is possible to

investigate whether the ozone-induced reduction in photosynthetic rates of leaves of varying maturity might be enough to account for the observed change in carbon allocated to roots, stems and leaves, and subsequent changes in measured growth parameters.

Further scaling from individual tree to simulate a ‘patch’ of trees composed of different genotypes may be used to investigate the interactive effects of elevated [CO₂] and [O₃] on forest growth and composition, under both limiting and non-limiting conditions, via competitive and species distribution response (Host et al., 1996; Kirschbaum, 2000). Future work to produce robust models of such complexity will require the co-operation of interdisciplinary teams of experimentalists, physiologists, modellers and programmers (Isebrands and Burk, 1992). Each stage of the scaling process will require model testing and validation (Jarvis, 1995).

The focus of this paper is to test the scaling of an ozone model from the leaf level to the whole tree level for the ozone-sensitive aspen clone 259. This is a first step in building a model to simulate the effects of atmospheric and climate change on carbon sequestration potential of a forest stand via competitive effects within a stand of trees. To this end, a model developed to predict the effects of ozone on photosynthesis and stomatal conductance has been incorporated into the functional-structural tree growth model ECOPHYS (Rauscher et al., 1990; Host et al., 1996; Isebrands et al., 2000; ECOPHYS web site: <http://www.nrri.umn.edu/ecophys>).

The process-based ozone model originally used the linear relationship between the maximum capacity of in vivo carboxylation (V_{cmax}) and effective ozone dose, based on an accumulated dose above a threshold flux of ozone entering the leaf, to calculate the relative effect of ozone on wheat leaf photosynthesis (Martin et al., 2000). The model was first developed within WIMOVAC (Windows Intuitive Model of Vegetation response to Atmosphere and Climate Change) (Humphries and Long, 1995) and determined net CO₂ assimilation rates via coupled mechanistic, biochemical model equations of photosynthesis (Farquhar et al., 1980; von Caemmerer and Farquhar, 1981) and stomatal conductance (Ball et al., 1987, adapted by Harley et al., 1992).

Incorporation of the ozone model and the coupled photosynthesis and stomatal conductance model equations into the functional-structural tree growth model ECOPHYS integrates physiological processes with the architectural attributes of a tree canopy and incorporates the numerous feedback mechanisms that occur among individual plant components (Host, 1990a; Host et al., 1999). Simulations from whole systems models, that include detailed component process sub-models, have the potential to be extrapolated beyond the conditions used for model development (Reynolds et al., 1993).

The objectives of the present study are threefold. First, to scale the ozone effect model to the whole tree level by incorporating the recently developed process-based model to predict the effects of ozone on photosynthesis into the object-oriented functional and structural tree growth model ECOPHYS (Isebrands et al., 2000). Second, to parameterise the model to simulate the growth of aspen clone 259 exposed to episodic variation in ozone during 1991, based on data of Karnosky et al. (1996). And, finally, to test the tree growth simulation against field results under square-wave exposure to ozone. The extent to which observed relative ozone response of aspen growth and whole tree carbon allocation can be attributed to effects on photosynthesis is discussed. Further model development, planned to reduce predictive uncertainty, is summarised.

2. Methods

2.1. ECOPHYS-ozone model

ECOPHYS was developed to simulate the growth of hybrid poplar and aspen clones over multiple years under interacting environmental stresses by integrating information on canopy architecture, leaf light interception and photosynthetic rate, root distribution and a dynamic process model of carbon allocation. Environmental inputs to the model include latitude, solar radiation, air temperature, relative humidity and ambient concentrations of both carbon dioxide and ozone. Individual leaves and root segments are defined in a three-dimensional co-ordinate system, allowing detailed calculations of hourly light interception for each leaf, and differential uptake of water and nutrients by roots in a heterogeneous soil environment. For this study ECOPHYS is used to simulate the growth of a single tree in the first establishment year, on an hourly time-step, assuming optimal water and nutrient availability.

2.1.1. Shading

Direct beam solar radiation intercepted by each leaf in a given hour is calculated within ECOPHYS from solar altitude and azimuth, according to leaf angle and leaf position relative to the sun, and shading from other leaves (Isebrands et al., 2000). Each upper-leaf surface is represented by a two-dimensional quadrilateral with bilateral symmetry (kite shape), with general leaf shape, for example, lance, flaring, square, or stubby, defined by parameters listed in the genetic library.

The shaded fraction of each leaf is calculated at each hourly time step. The four vertices of each leaf are located within an x - y - z co-ordinate system, where the z axis is parallel to a vector from the earth to the sun. The leaf with the smallest z value is above all the other leaves (Fig. 1). The four vertices of each leaf are projected onto

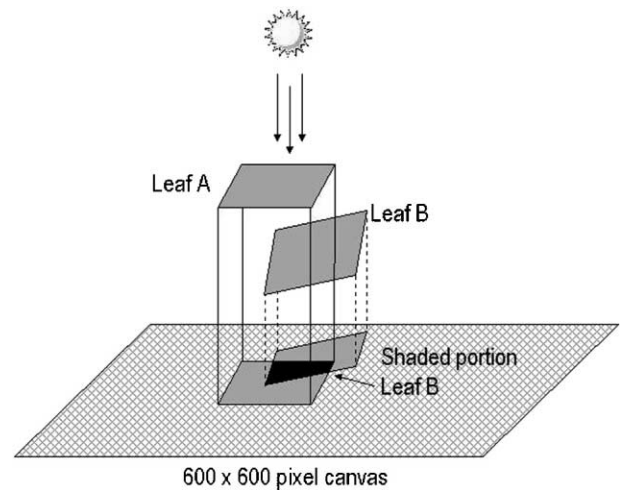


Fig. 1. The relationship between the radiation vector, leaves, and the 600×600 pixel canvas (adapted from Zhao, 2000a).

a plane perpendicular to the sun vector, represented by a 600×600 pixel area termed the canvas (Wu, 1999).

A list of all the leaves is sorted in ascending order according to leaf centre point z values. If a pixel is shaded, the corresponding element of the 600×600 array is set to 1, otherwise, it is 0. Starting from the first leaf in the list, the four vertices of each leaf are projected onto the canvas. In the projected region for the leaf, the number of shaded pixels is compared to the total number of pixels covered by the leaf's projection to determine the fraction of the leaf that is shaded. Then all the pixels covered by the leaf's projection are marked as shaded for calculating the shaded area of the next leaf (Zhao, 2000a).

2.1.2. Photosynthesis

Photosynthetic rate is calculated in response to hourly inputs of photon flux density, air temperature, relative humidity and ambient concentrations of CO_2 and O_3 for both the sunlit and shaded portions of the leaf. Given that the simulations represent only the first year of growth, and that there is no mutual shading from adjacent trees, foliar nitrogen levels are assumed to be optimum for the purposes of this study. For each leaf, photosynthetic rates for sunlit and shaded areas are multiplied, respectively, by the sunlit and the shaded leaf area and summed to determine total photosynthate production for the leaf at each hourly time step. For this study ECOPHYS uses the coupled photosynthesis and stomatal conductance model developed for WIMOVAC (Humphries and Long, 1995), parameterised for aspen and modified to account for leaf age and O_3 damage.

Within WIMOVAC net CO_2 assimilation rates are calculated by combining the well-accepted mechanistic biochemical model equations for photosynthesis developed by Farquhar et al. (1980) and von Caemmerer and Farquhar (1981) and adapted to account for

phosphorylation-limited rate (Sharkey, 1985), with the phenomenological model equations of stomatal conductance (Ball et al., 1987, adapted by Harley et al., 1992). Values for net CO₂ assimilation and stomatal conductance are solved through an iterative process.

Although the same equations were used in ECO-PHYS to calculate assimilation rates, the equations were solved analytically. The analytical solution (Zhao, 2000b) was derived as in Baldocchi (1994), although mathematical expressions differ somewhat from those in Baldocchi (1994). In particular, a phosphate limitation on photosynthetic rate was included. As in Baldocchi (1994), the system of equations is solved analytically by expressing photosynthetic rate as the minimum among roots of quadratic and cubic polynomials. The expressions for the roots are complicated, but are evaluated quickly by computer. To verify that the analytical method was implemented correctly, it was extensively tested against the iterative method (Zhao, 2000b). The two were found to coincide both at the leaf-level and at the whole-tree level when simulations were run under normal ranges of environmental conditions.

The analytical calculations require a fixed amount of time whereas the time taken by the iterative method depends on operating conditions. Under typical environmental conditions, the iterative method was found to be approximately as fast as the analytical method. However, for some environmental conditions many iterations are needed and outside certain ranges the iterative method may not converge. Also, performance of the iterative method depends on parameter values that vary with plant species and ozone damage.

2.1.3. Ozone model

The ozone model incorporated into ECOPHYS was adapted from the process-based model developed to predict the photosynthetic response of wheat to acute ozone exposure, based on the data from Farage et al. (1991) (Martin et al., 2000). Model equations are

Table 1

Model equations to simulate the effects of ozone exposure on rates of photosynthesis in aspen clone 259

$$F'_{O_3\text{eff}} = \int_0^t ([O_3] \cdot g_z) - F_{O_3(0)} \cdot dt \quad (1)$$

$$g_z = g_s / 1.67 \quad (2)$$

$$g_s = g_{(0)} + g_{(1)} \cdot (A \cdot R_H / C_a) \quad (3)$$

$$\Delta V_{\text{cmax}} = K_z \cdot F'_{O_3\text{eff}} \quad (4)$$

$$\Delta V_{\text{cmax}} = K_z \cdot F'_{O_3\text{eff}} \quad (5)$$

listed in Table 1 and symbols defined in Table 2. The underlying mechanism of the ozone-inhibited photosynthesis model is that damage occurs once the protective scavenging detoxification system is overloaded, above a critical flux of ozone entering the leaf (Heath, 1994). The model uses the linear relationship between the relative reduction in V_{cmax} and the 'effective ozone dose' ($F'_{O_3\text{eff}}$), that is, the accumulated amount of ozone entering the leaf above the threshold flux ($F_{O_3(0)}$), to calculate the effect of ozone exposure on leaf photosynthesis. The threshold flux is related to the maximum capacity of scavenging protective metabolism within the leaf. The slope coefficient of the linear function, K_z , reflects the sensitivity of the photosynthetic apparatus to ozone above the threshold flux. This occurs once the maximum rate of protective metabolism against active oxygen radicals has been exceeded. This linear relationship is then used to determine the dependence of ozone-induced stomatal closure on V_{cmax} , via intercellular [CO₂] (c_i).

Thus, the wheat ozone model predicts stomatal closure caused by ozone exposure, via its effect on V_{cmax} [Eqs. (1)–(4), Table 1], where g_z is the stomatal conductance to ozone and g_s is the stomatal conductance to water, calculated by Eq. (3), using the method of Ball et al. (1987), as adapted by Harley et al. (1992). Ozone enters both wheat and aspen leaves via the stomata, and, like wheat, the V_{cmax} of ozone-sensitive aspen (clone 259) is reduced by exposure to ozone (Kull et al., 1996). However, ozone was also found to reduce the light-saturated rate of electron transport, J_{max} , in leaves of clone 259 [Eq. (5), Table 1] (Kull et al., 1996). Evidence of this additional effect of high doses of ozone on photosynthesis has also been found in other woody species, such as oak (Farage and Long, 1995). The proposed leaf-level model of ozone effects on aspen is outlined in Fig. 2.

Over extended periods of ozone exposure visible ozone symptoms occur. For this study it is assumed that any loss of green leaf area due to necrosis and stippling observed in aspen leaves results from the loss of photosynthetic capacity and is accounted for as a loss of photosynthetic capacity in the model.

2.1.4. Carbon allocation and growth

Translocation of photosynthate to various parts of the tree is achieved according to detailed carbon allocation matrices based on carbon tracing measurements (Host et al., 1990a, 1996; Rauscher et al., 1990). Each leaf in the canopy has a carbon transport pattern based on LPI (leaf plastochron index) (Larson and Isebrands, 1971). Newly emerged leaves (LPI 1–4) retain all of their photosynthate, whilst leaves in the expanding leaf zone (LPI 5–9) transport most of their photosynthate upward to leaves and stem internodes, and mature leaves (LPI > 10) transport most of their photosynthate

Table 2
Definition of symbols and parameter values of the combined ozone/photosynthesis model

| Term | Value | Units | Definition and source |
|-----------------------------|-------|--------------------------------------|------------------------------------------------------------------------------------------|
| A | | $\mu\text{mol m}^{-2} \text{s}^{-1}$ | Net leaf rate of CO_2 uptake per unit leaf area |
| C_a | 350 | $\mu\text{mol mol}^{-1}$ | Atmospheric concentration of CO_2 |
| $F'_{\text{O}_3\text{eff}}$ | | mmol m^{-2} | Effective ozone dose |
| $F_{\text{O}_3(0)}$ | 9 | $\text{nmol m}^{-2} \text{s}^{-1}$ | Threshold flux of ozone entering the leaf |
| g_s | | $\text{mmol m}^{-2} \text{s}^{-1}$ | Stomatal conductance to water |
| g_z | | $\text{mmol m}^{-2} \text{s}^{-1}$ | Stomatal conductance to ozone (Laisk et al., 1989) |
| g_0 | 81.1 | Dimensionless | Minimum stomatal conductance to water when $A=0$ at light compensation point |
| g_1 | 9.58 | Dimensionless | Empirical coefficient of stomatal conductance sensitivity to A , C_a , and R_H |
| J_{max} | 162 | $\mu\text{mol m}^{-2} \text{s}^{-1}$ | Light saturated rate of potential rate of electron transport |
| K_z | 8.35 | Dimensionless | Empirical coefficient of sensitivity of V_{cmax} to $F'_{\text{O}_3\text{eff}}$ |
| R_H | | % | Relative humidity |
| V_{cmax} | 101 | $\mu\text{mol m}^{-2} \text{s}^{-1}$ | Maximum RuBP saturated rate of carboxylation |

downward to stem internodes, trunk, and root. The carbon transport coefficients for active, unstressed growth were determined by ^{14}C tracer studies in controlled environments and in the field (Larson, 1977; Isebrands and Nelson, 1983; Dickson, 1986; Host et al., 1990a).

After budset, carbon allocation patterns change as active growth gives way to preparation for winter. This is simulated in ECOPHYS by a linear interpolation of active growth carbon allocation matrices to end of season storage carbon allocation matrices (Host et al., 1990b). During the 10 days centred around budset, linear interpolation is used to gradually decrease the upward leaf and internode transportation coefficients from 100 to 20% of their active growth values, with the corresponding increase in carbon allocated to lower stem and root tissues (Zang, 1999).

The below ground component of ECOPHYS simulates movement of water and nutrients in three-dimensional space as a function of soil water potential, and allows for differential uptake by a heterogeneous three-dimensional root growth submodel (Theseira et al., 2001). Root architecture is based on a relaxed fractal algorithm for carbon allocation coupled with genetically determined branching rules. Roots are tracked by position and order using a tree structure (Host et al., 1996). The growth process is simulated by incremental increases in photosynthate allocated to the leaf, internode and root sinks on an hourly basis, accounting for temperature effects and respiratory losses.

2.1.5. Growing season leaf-drop algorithm

Increasing levels of ozone exposure can increase leaf senescence during the growing season. The simulation of leaf senescence during the growing season is based on the productivity of each leaf. For each leaf the net photosynthate per unit leaf area remaining after respiration and reallocation is averaged over 10 days. If this average falls below a threshold value, then, with a

certain probability, the leaf drops. Full details of the leaf-drop algorithm are presented in the Appendix.

ECOPHYS model outputs are: leaf count, leaf area (cm^2), stem height (cm), stem diameter (cm), leaf dry weight (g), stem dry weight (g), cumulative whole-tree dry matter production (g), root length (cm) and dead leaf matter production (g).

2.2. Model development and parameterisation

2.2.1. Clonal library

The clone library file of ECOPHYS contains values for genetic input parameters, originally determined for hybrid poplar (*Populus × euramericana*) ‘Eugenei’, but altered for this work to represent aspen clone 259 (Host et al., 1990b; 1996). The clonal library parameter values are listed in Table 3.

2.2.2. Leaf maturity class effects on photosynthesis

Kull and co-workers (1996) found that for leaves of aspen clone 259, light-saturated rates of photosynthesis reached maximum values only above LPI 11, and that ozone had no effect on leaves of LPI less than 11 (Fig. 3). Therefore, the leaf maturity class effects on photosynthetic rate and ozone response were adapted in ECOPHYS according to the reported data, whereby the maximum photosynthetic rates for leaves of LPI less than 11 was linearly related to LPI by Eq. (6), and the ozone model was not used for leaves with an LPI value of less than 11 (Fig. 3).

$$A_{\text{ratiotoLPI}} = 1.161 \cdot \text{LPI} + 2.625 \quad (6)$$

2.2.3. Model input and parameter values

Air temperature and relative humidity values recorded in Karnosky’s 1991 experiments were used as inputs to the simulation (Karnosky et al., 1996). Photon flux density was simulated by model equations using the

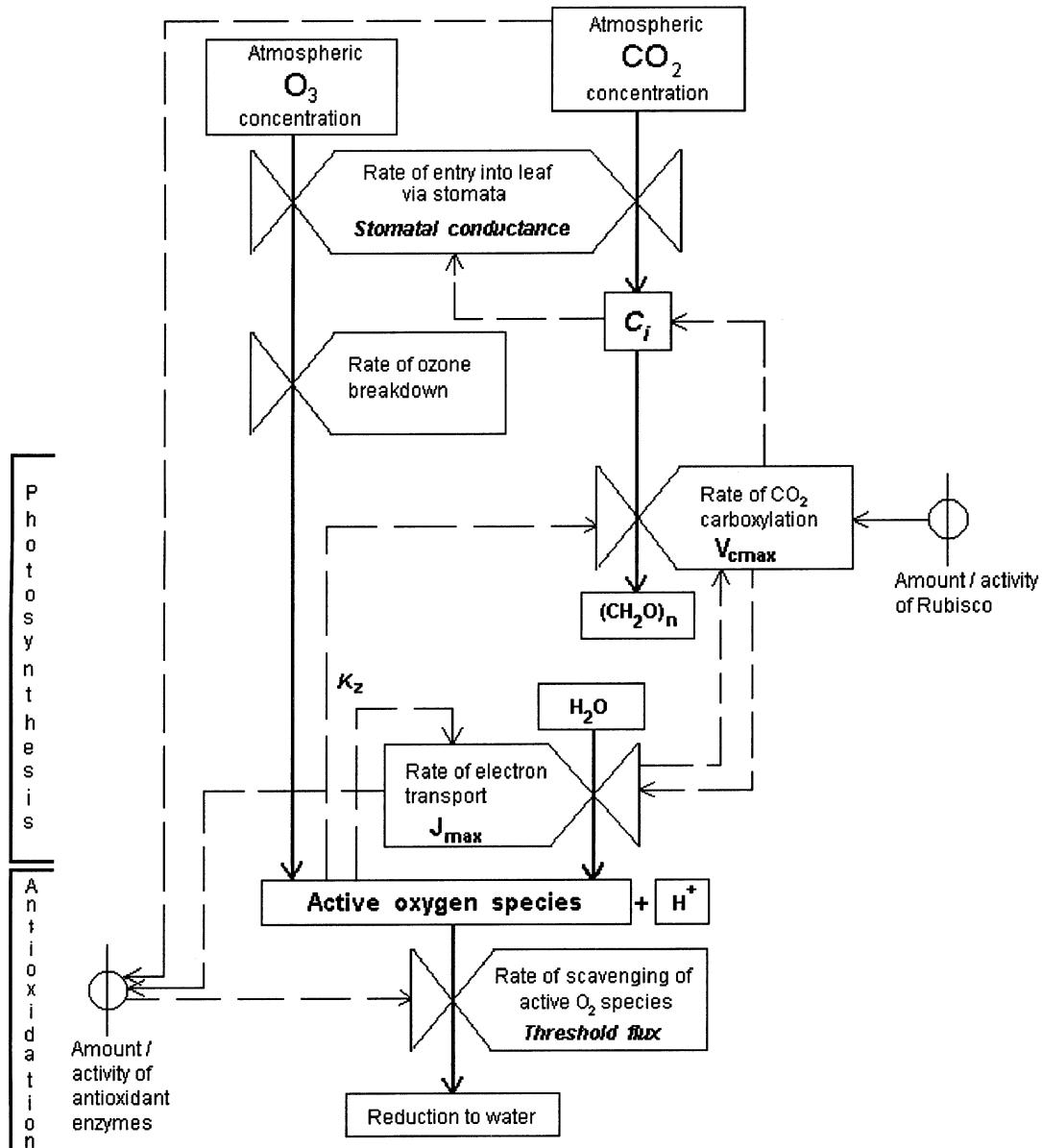


Fig. 2. Schematic of the ozone model for aspen, including effect on J_{\max} .

latitude 46° N and ambient [CO₂] was set at 350 μmol m⁻² s⁻¹. Input variation of ozone concentration were those values targeted by the experiments of Karnosky et al. (1996). Ozone treatments simulated consisted of charcoal filtered (CF) and an episodic 'two times' ozone concentration (2×), based on a doubling of hourly ambient ozone concentrations measured in Michigan's Lower Peninsula (Hoggsett et al., 1988).

Carboxylation efficiency and A_c curve data for aspen clone 259 grown in open-top chambers under various ozone treatments (Kull et al., 1996) were used to determine mean $V_{c\max}$ and J_{\max} values, and to provide a first estimate of ozone parameter values. The value of the ozone sensitivity coefficient (K_z) was adjusted from that found using the data of Kull et al. (1996) to reflect the relative reduction in stem dry matter production

observed between 2× and CF treatments measured in experiments conducted in 1991 by Karnosky et al. (1996). Parameter values are listed in Table 2 (Fig. 3). The model would then be tested against separate growth data of aspen grown in 1991 under the square wave ozone exposure regime used by Karnosky et al. (1996).

2.3. Model testing

To test the model, the results of an ECOPHYS simulation of growth response of aspen clone 259 grown in open-top chambers in 1991 by Karnosky et al. (1996) under square wave ozone profile were compared with the observed changes in growth parameters, including stem diameter, stem height, and total leaf area. The square-wave (SQ) variation of ozone concentration

Table 3
Clonal library parameter values for aspen clone 259

| Parameter description | Value (units) |
|------------------------------------------------|--------------------------------------------|
| Bud break date | 128 (Julian day) |
| Bud set date | 233 (Julian day) |
| Leaf senescence date | 268 (Julian day) |
| Leaf initiation rate | 36 (number of days) |
| Leaf senescence rate | 3 (number of days) |
| Initial expanding leaf zone specific leaf area | 0.2222 (cm ² mg ⁻¹) |
| Budset expanding leaf zone specific leaf area | 0.159 (cm ² mg ⁻¹) |
| Internode specific gravity | 0.46 (g cm ⁻³) |
| Ratio of leaf width to leaf length | 1 |
| Growth respiration rate | 0.250 (ratio) |
| Maintenance respiration rate | 0.015 (day ⁻¹) |

consisted of exposure to [O₃] of 100 nmol mol⁻¹ for 6 h a day, for 4 days a week, for a total of 12 weeks.

3. Results

Model simulations of the relative growth response of ozone-sensitive aspen clone 259 under ozone exposure, compared with the charcoal filtered treatment, reflect the general trends reported by Karnosky and co-workers. In particular, the model showed that: (1) stem dry matter production and stem diameter are dramatically reduced by ozone, while the effect on stem height was small (Fig. 4a–c); (2) ozone-induced earlier leaf abscission dramatically reduces both leaf dry matter production and retained leaf area, but with little or no effect on the number of leaves initiated (Fig. 5a–c); (3) decline in root growth is one of the most sensitive indicators of chronic ozone exposure (Fig. 6) (Karnosky et al., 1996). The predicted reduction in stem dry matter production was within 2% of that measured by Karnosky et al. (1996). A drop of 40% in total root length was simulated (Fig. 6), whereas Karnosky et al. (1996) measured a 55% reduction in root dry matter production, with exposure to 2×. The simulated percentage reduction in retained leaf biomass under 2× ozone treatment depended on the date (Fig. 5a) and varied between 17 and 30%. The measured reduction was 36%.

The square wave ozone profile was used to test the model. Simulated responses to square wave treatment are of a similar order to those of the 2× treatment, even though the total ozone supplied for the whole experimental period of the 2× treatment was calculated by Karnosky et al. (1996) to be nearly twice as high as that of the SQ treatment. This agrees with the similar response between square wave and 2× treatments measured by Karnosky et al. (1996) although slightly lower reductions in response were measured under square wave exposure, simulated as slightly greater reductions by ECOPHYS (Fig. 4–6). Once again, only a 40% drop in root length was simulated (Fig. 6), although a 53%

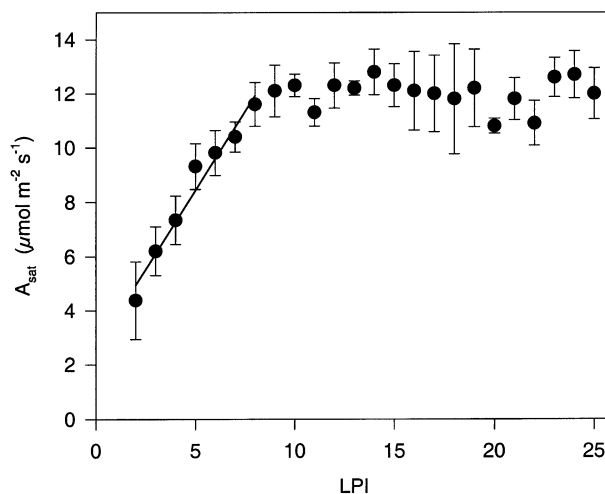


Fig. 3. Relationship between light-saturated rate of photosynthesis and leaf plastochron index for aspen clone 259 (after Kull et al., 1996).

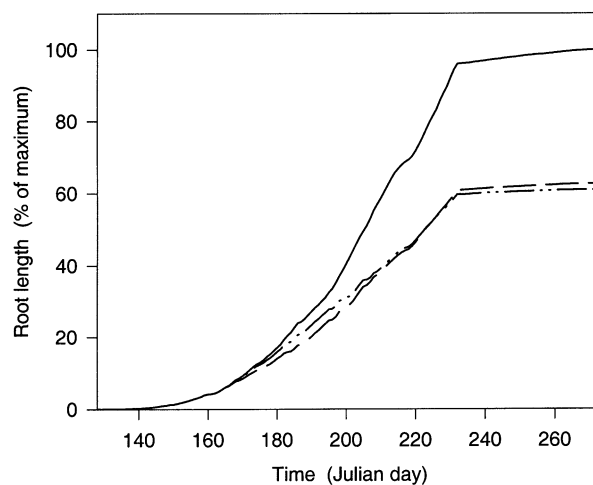


Fig. 4. Simulations of aspen clone 259 stem: (a) dry matter production; (b) diameter; and (c) height under exposure to different ozone treatments: CF (—), 2× (---) and SQ (-·-·-).

reduction in root biomass was measured by Karnosky et al. (1996) at the end of the growing season. Leaf dry matter production was predicted to drop by between 20 and 37%, depending on date, compared with a measured reduction of 32% under ozone regime SQ.

4. Discussion

The model presented here combines validated leaf-level sub-models within a functional and a structural tree growth model to increase our understanding of scaling processes from leaf to whole tree level. The model incorporates a process-based model to predict photosynthetic response to ozone (Martin et al., 2000), the combined stomatal conductance (Ball et al., 1987; Harley et al., 1992) and mechanistic models of CO₂ assimilation (Farquhar et al., 1980; von Caemmerer and

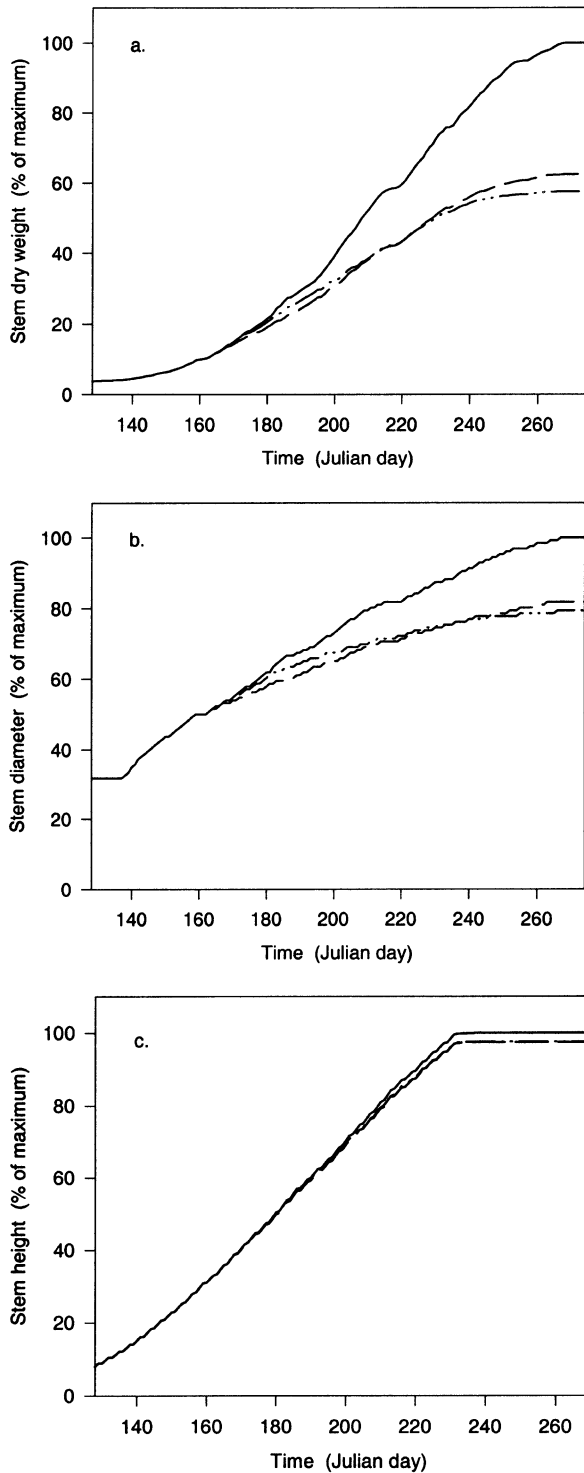


Fig. 5. Simulations of aspen clone 259 leaf: (a) dry matter production; (b) area; and (c) number of leaves initiated, under exposure to different ozone treatments: CF (—), 2 \times (---) and SQ (— · — ·).

Farquhar, 1981; Sharkey, 1985), within a detailed light interception model of tree growth (Rauscher et al., 1990; Host et al., 1990a, 1996, 1999; Isebrands et al., 2000). Working on an hourly time step, this composite, mechanistic approach allows this revised version of

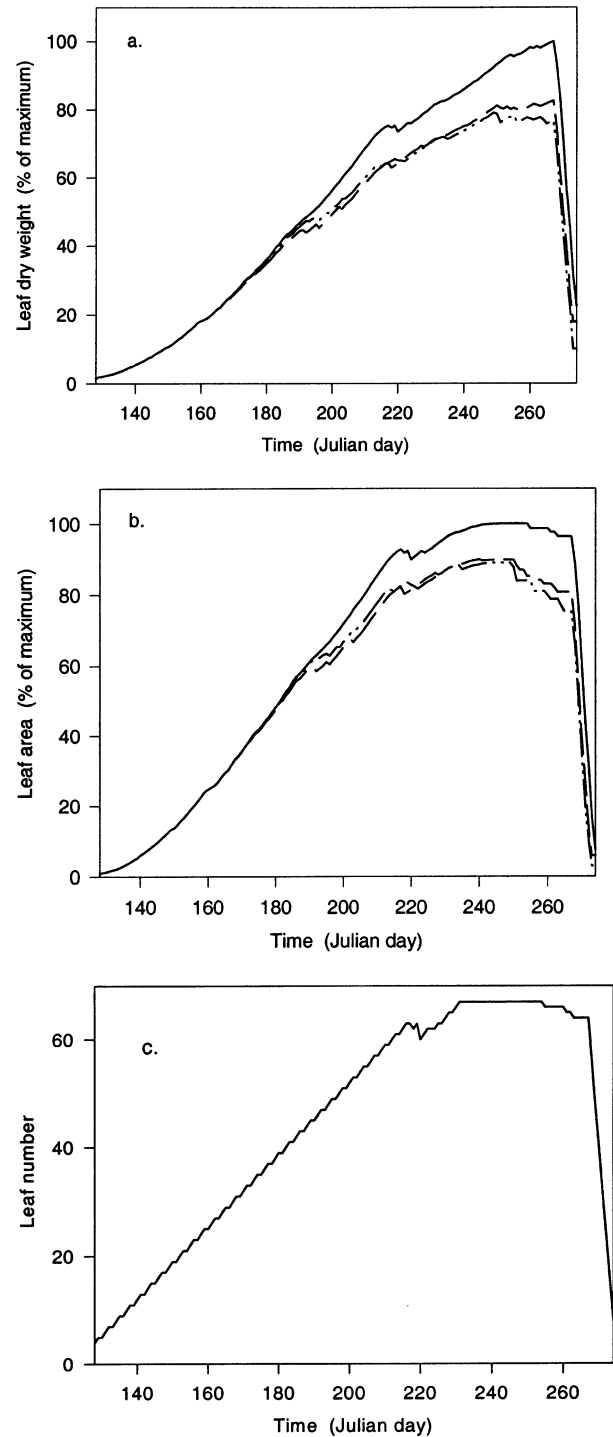


Fig. 6. Simulations of aspen clone 259 root length under exposure to different ozone treatments, CF (—), 2 \times (---) and SQ (— · — ·).

ECOPHYS to simulate the observed relative response of above ground growth of ozone-sensitive aspen clone 259 to one season's exposure to ozone. Model simulations concur with observations that ozone affects aspen growth parameters differentially. Stem dry matter production and stem diameter are reduced dramatically, whereas ozone has a relatively small effect on stem

height (Fig. 4). Also, whilst both leaf biomass and leaf area are sensitive to ozone, the number of leaves initiated is unaffected (Fig. 5). These findings support the scaling method employed here, whereby process-based models of ozone effects and photosynthesis at the leaf level are incorporated into a structural-functional tree growth model to simulate the observed effects on above ground dry matter production of an ozone-sensitive aspen clone.

A direct comparison between simulated and observed effects on aspen clone root growth is not possible at this stage, as the present version of ECOPHYS simulates root growth in terms of root length, and not root dry matter production, as measured by Karnosky et al. (1996). A three-dimensional root growth and soil model component is currently being constructed for ECOPHYS (Theseira et al., 2001). Meanwhile, the predicted 40% reduction in root length may be interpreted as a reasonable simulation of the measured 55% reduction in root biomass when uncertainties due to the practical problems of root biomass measurement, possible sink restrictions by growth in pots and growth chamber effects are taken into account.

When tested against independent data for growth response under the square wave $[O_3]$ profile, ECOPHYS simulates a similar magnitude of reduction in ozone-sensitive growth parameters to those measured under the $2\times$ episodic exposure treatment, despite the difference between ozone regimes. The total seasonal ozone exposure under the square wave ozone profile is nearly twice that under the $2\times$ episodic ozone treatment, and the pattern of exposure and peak values of $[O_3]$ also differed markedly. This ability of the model to predict the similar magnitude of effects of the two ozone treatments supports the threshold flux concept when scaling results to the whole tree. The threshold flux, below which no damage occurs, reflects the maximum capacity of the protective oxidant scavenging system. The hourly time step of leaf level calculations and input values for $[O_3]$, $[CO_2]$, temperature, light and relative humidity allow CO_2 assimilation rates, stomatal conductance and ozone effects to be simulated on a physiologically realistic time scale [for a more detailed discussion of appropriate time steps for model simulations, see Constable and Friend (2000)].

The aim of this modelling exercise was to test the scaling of the model for predicting ozone effects on whole tree photosynthesis, and thus to investigate how much the observed ozone-induced reduction in carbon allocated to leaves, stems and roots may be accounted for solely by reduced photosynthetic rates. Coleman et al. (1995a) reported the ozone-induced reduction in total carbon translocated to sink tissue in aspen clone 259 to be controlled by reduced photosynthetic rates. ECOPHYS simulations that followed observed trends in the response of above ground dry matter production

of ozone-sensitive aspen to one season's exposure to ozone support this. The model predicts root length to be dramatically reduced (Fig. 6). The effects of ozone on the more mature leaves of the lower canopy, which are exposed to ozone for longer periods than less mature leaves, and export most of their assimilate down to the roots (Coleman et al., 1995a), helps to explain the ozone-sensitivity of root dry matter production.

Observed ozone-induced changes in allocation in other species have been attributed to other processes affecting allocation, such as phloem translocation, in addition to effects on CO_2 assimilation rates, as found in Pima cotton when exposed to acute ozone (see Grantz and Farrar, 1999). Grant and Farrar suggests effect on phloem translocation may be mediated by oxidation damage to membranes within intercellular air spaces, such as the plasmalemma and plasmodesmata of mesophyll and phloem companion cells. Therefore, although this model can simulate effects on growth of ozone-sensitive aspen via effects on photosynthesis, additional routines describing the ozone effects on carbon allocation might be needed to simulate growth response in other species. Perhaps the relationship between the ozone threshold flux $F_{O_3(0)}$ and the maximum capacity of the scavenging potential could also be useful for calculating ozone-induced reduced rates of carbon translocation in species where ozone is known to damage membranes within intercellular spaces.

Many uncertainties are introduced when scaling models, both temporally, from hours and days to months, and spatially, from a leaf to a whole tree. Uncertainties associated with the change in temporal scale include possible recovery from ozone damage and adaptation, and whether the mechanism for adaptation might occur by natural selection over several generations, an adjustment from one season's growth to the next, or a more immediate response, for example, by an increase in the capacity of protective scavenging mechanisms. This study concentrates on just one year's growth of aspen clone 259 under conditions where water and nitrogen are assumed to be non-limiting. Although a possible change in maximum capacity of the oxidative scavenging system with time of ozone exposure and leaf position should be investigated, initial evidence suggests the production of the anti-oxidants chloroplastic and cytosolic Cu/Zn superoxide dismutase, does not increase in ozone-sensitive clone 259 following O_3 exposure, contrary to the increase reported in ozone tolerant clones (Karnosky et al., 1998).

Therefore, whilst the results of this study support the suggestion that relative changes in above ground carbon allocation under ozone can be accounted for solely by changes in photosynthetic rates at the leaf level, via differential leaf age effects, earlier leaf abscission and resulting changes in carbon allocation, uncertainties in simulating and measuring effects on root carbon

gain need to be resolved, particularly when further scaling the model to predict ozone effects on a stand of trees, over multiple years. Not only will the effects of ozone over several successive years need to be taken into account, but also the effects of mutual shading of leaves within the stand, and competition for light, water and nitrogen effects on ozone uptake.

Understanding how much the response of forest biomass production and carbon sequestration capacity to climate and atmospheric change might be influenced by effects on competitive and species distribution within a forest stand (Kirschbaum, 2000) will require robust detailed models to compare simulated changes in biomass via effects on genotype composition, with simulations of biomass changes from more generic models of a forest canopy. Care must also be taken when using models based on seedling studies to try to predict effects on mature trees (Kolb et al., 1997). Future work is planned to scale the model further, from the individual tree to the level of a patch of trees of known age and of known genotype composition (Host et al., 1996). ECOPHYS is currently being adapted to enable model simulations of tree growth over several seasons. Not only will this require adaptation to incorporate the possible over-winter effects of ozone on bud break and branching, but it will also require adjustment to simulate season-to-season variability in branch budding under non-stressed conditions. To overcome limitations imposed by running such large simulations on processor time, the use of component object modelling (COM) is being developed for ECOPHYS, to allow simulations to be conducted across parallel computers (Isebrands et al., 2000).

Meanwhile, the results of this study support the method of incorporating process-based leaf level models into whole tree growth models to further understand processes at the whole tree level. The findings support Coleman et al.'s (1995a) suggestion that the above ground growth response of ozone-sensitive aspen to ozone exposure can be accounted for by the direct effects of ozone on photosynthesis.

Acknowledgements

We would like to extend our thanks to M.D. Coleman, A. Sober, E. McDonald and A. Noormets for useful discussions on aspen data and W. Zhao for programming support. We acknowledge Steve Long and Steve Humphries for background information on the formulation of the model WIMOVAC. Work on the original ozone model was funded by the Natural Environmental Research Council, UK, under grant GT4/92/16/L; initial parameterization of the model for aspen clones was funded by a grant to the University of Essex, from Brookhaven National Laboratory. Development

of the ECOPHYS project was funded jointly by the Computational Biology Program of the National Science Foundation, Grant No. DBI-972395, the Northern Global Change Program of the USDA Forest Service, and the US Department of Energy under inter-agency agreement No. DE-A105-800R20763. Additional funding came from the NSF/DOE/NASA/USDA Joint Program on Terrestrial Ecology and Global Change through a co-operative agreement with Michigan Technological University. This is Contribution No. 296 of the Center for Water and the Environment, Natural Resources Research Institute, University of Minnesota–Duluth.

Appendix. Growing season leaf-drop algorithm

For each leaf on any given day d denote gross photosynthate produced by the leaf by $P_g(d)$, leaf maintenance respiration by $R_m(d)$, photosynthate transported out of the leaf by $P_t(d)$, photosynthate received from other leaves by $P_r(d)$, leaf growth respiration by $R_g(d)$, and leaf area by $A_L(d)$. Net photosynthate produced per unit leaf area for a given leaf on day d , $P_{n/a}(d)$, is computed as follows.

$$P_{n/a}(d) = \frac{[(P_g(d) - R_m(d)) - P_t(d) + P_r(d)] - R_g(d)}{A_L(d)}$$

The parentheses are necessary because $P_t(d)$ is based on $(P_g(d) - R_m(d))$ as well as on leaf age. Likewise, $R_g(d)$ is based on

$$((P_g(d) - R_m(d)) - P_t(d) + P_r(d))$$

as well as on leaf age.

For each leaf for each day, beginning on the 10th day since the leaf's emergence, the net photosynthate per unit leaf area is averaged over the current day together with the previous nine days. That is,

$$Pa_{n/a}(d) = \frac{(P_{n/a}(d) + P_{n/a}(d-1) + \dots + P_{n/a}(d-9))}{10}$$

Denote the threshold value for $Pa_{n/a}(d)$, below which the leaf might drop, by τ . Define $K = (Pa_{n/a}(d) - \tau) * \delta$. Here, τ is a measure of leaf starvation and δ is a scaling factor affecting the likelihood that a starving leaf will drop. In this study, $\tau = 0$ and $\delta = 3$, although the values of τ and δ vary among genotypes. Let ξ denote a uniform random number such that $0 \leq \xi \leq 1$. Whether or not a given leaf drops on a given day d is determined by the following algorithm:

If $K \geq 0$ the leaf remains, else if $\xi > 1 - e^K$ the leaf remains, else the leaf drops.

Here, ξ is used to simulate uncertainty and variability due to unmodeled dynamics. The probability that a leaf drops when $Pa_{n/a}(d) < K$ is $1 - e^{-K}$.

References

- Baldocchi, D., 1994. An analytical solution for coupled leaf photosynthesis and stomatal conductance models. *Tree Physiology* 14, 1069–1079.
- Ball, J.T., Woodrow, I.E., Berry, J.A., 1987. A model predicting stomatal conductance and its contribution to the control of photosynthesis under different environmental conditions. In: Biggins, I. (Ed.), *Progress in Photosynthesis Research*, Vol. IV. Proceedings of the International Congress on Photosynthesis. Martinus Nijhoff, Dordrecht, pp. 221–224.
- Chameides, W.L., Kasibhatla, P.S., Yienger, J., Levy II, H., 1994. Growth of continental-scale metro-agro-plexes, regional ozone pollution and world food production. *Science* 264, 74–77.
- Coleman, M.D., Isebrands, J.G., Dickson, R.E., Karnosky, D.F., 1995a. Photosynthetic productivity of aspen clones varying in sensitivity to tropospheric ozone. *Tree Physiology* 15, 585–592.
- Coleman, M.D., Dickson, R.E., Isebrands, J.G., Karnosky, D.F., 1995b. Carbon allocation and partitioning in aspen clones varying in sensitivity to tropospheric ozone. *Tree Physiology* 15, 593–604.
- Constable, J.V.H., Friend, A.L., 2000. Suitability of process-based tree growth models for addressing tree response to climate change. *Environmental Pollution* 110, 47–59.
- Dickson, R.E., 1986. Carbon fixation and distribution in young *Populus* trees. In: Fujimori, T., Whitehead, D. (Eds.), *Proceedings, Crown and Canopy Structure in Relation to Productivity*. Forestry and Forest Products Research Institute, Ibaraki, Japan, pp. 409–426.
- Farage, P.K., Long, S.P., Lechner, E.G., Baker, N.R., 1991. The sequence of change within the photosynthetic apparatus of wheat following short-term exposure to ozone. *Plant Physiology* 95, 529–535.
- Farage, P.K., Long, S.P., 1995. An *in vivo* analysis of photosynthesis during short-term O₃ exposure in three contrasting species. *Photosynthesis Research* 43, 11–18.
- Farage, P.K., 1996. The effect of ozone fumigation over one season on photosynthetic processes of *Quercus robur* seedlings. *New Phytologist* 134, 279–285.
- Farage, P.K., Long, S.P., 1999. The effects of O₃ fumigation during leaf development on photosynthesis of wheat and peas: an *in vivo* analysis. *Photosynthesis Research* 59, 1–7.
- Farquhar, G.D., von Caemmerer, S., Berry, J.A., 1980. A biochemical model of photosynthetic CO₂ assimilation in leaves of C₃ species. *Planta* 149, 78–90.
- Grantz, D.A., Farrar, J.F., 1999. Acute exposure to ozone inhibits rapid carbon translocation from source leaves of Pima cotton. *Journal of Experimental Botany* 50, 1253–1262.
- Harley, P.C., Thomas, R.B., Reynolds, J.F., Strain, B.R., 1992. Modelling photosynthesis of cotton grown in elevated CO₂. *Plant, Cell and Environment* 15, 271–282.
- Heath, R.L., 1987. Biochemical mechanisms of pollutant stress. In: Heck, W.W., Taylor, O.C., Tingey, D.T. (Eds.), *Assessment of Crop Loss from Air Pollutants*. Elsevier Science, London, pp. 259–286.
- Heath, R.L., 1994. Possible mechanisms for the inhibition of photosynthesis by ozone. *Photosynthesis Research* 39, 439–451.
- Hoggsett, W.E., Tingey, D.T., Lee, E.H., 1988. Ozone exposure indices: concepts for development and evaluation of their uses. In: Heck, W.W., Taylor, O.C., Tingey, D.T. (Eds.), *Assessment of Crop Loss from Air Pollutants*. Elsevier Science, London, pp. 107–137.
- Host, G.E., Rauscher, H.M., Isebrands, J.G., Michael, D.A., 1990a. Validation of photosynthate production in ECOPHYS, an ecophysiological growth process model of *Populus*. *Tree Physiology* 7, 283–296.
- Host, G.E., Rauscher, H.M., Isebrands, J.G., Dickmann, D.I., Dickson, R.E., Crow, T.R., Michael, D.A., 1990b. The Microcomputer Scientific Software Series No. 6: The ECOPHYS User's Manual (USDA Forest Service General Technical Report, NC-141).
- Host, G.E., Isebrands, J.G., Theseira, G.W., Kiniry, J.R., Graham, R.L., 1996. Temporal and spatial scaling from individual trees to plantations: a modeling strategy. *Biomass and Bioenergy* 11, 233–243.
- Host, G.E., Theseira, G.W., Heim, C., Isebrands, J.G., Graham, R., 1999. EPIC-ECOPHYS: a linkage of empirical and process models for simulating poplar plantation growth. In: Amaro, A., Tome, M. (Eds.), *Empirical and Process Models for Forest Tree and Stand Growth Simulation*, Edicos Salamandra, pp. 419–429.
- Humphries, S.W., Long, S.P., 1995. WIMOVAC: a software package for modelling the dynamics of plant leaf and canopy photosynthesis. *CABIOS Computer Applications in BioSciences* 11, 361–371.
- IPCC, 1996. Technical summary. In: Houghton, J.T., Meira Filho, L.G., Callander, B.A., Harris, N., Kattenberg, A., Maskell, K. (Eds.), *IPCC: Climate Change 1995*. Cambridge University Press, Cambridge, pp. 9–51.
- Isebrands, J.G., Burk, T.E., 1992. Ecophysiology growth process models of short rotation forest crops. In: Mitchell, C.P. (Ed.), *Ecophysiology of Short Rotation Forest Crops*. Elsevier Applied Science, London, pp. 231–266.
- Isebrands, J.G., Nelson, N.D., 1983. Distribution of [14C]-labeled photosynthates within intensively cultured *Populus* clones during the establishment year. *Physiologia Plantarum* 59, 9–18.
- Isebrands, J.G., Host, G.E., Lenz, K.E., Wu, G., Stech, H.W., 2000. Hierarchical, parallel computing strategies using component object model for process modeling responses of forest plantations to interacting multiple stresses. In: Cuelmans, R.J.M., Veroustraete, F., Gond, V., Van Rensbergen, J.B.H.F. (Eds.), *Forest Ecosystem Modeling, Upscaling, and Remote Sensing*. SPB Academic Publishing, The Hague, The Netherlands, pp. 123–135.
- Jarvis, P.J., 1995. Scaling processes and problems. *Plant, Cell and Environment* 18, 1079–1089.
- Karnosky, D.F., Gagnon, Z.E., Dickson, R.E., Coleman, M.D., Lee, E.H., Isebrands, J.G., 1996. Changes in growth, leaf abscission, and biomass associated with seasonal tropospheric ozone exposures of *Populus tremuloides* clones and seedlings. *Canadian Journal of Forestry Research* 26, 23–37.
- Karnosky, D.F., Podila, G.K., Gagnon, Z., Pechter, P., Akkapeddi, A., Sheng, Y., Riemenschneider, D.E., Coleman, M.D., Dickson, R.E., Isebrands, J.G., 1998. Genetic control of responses to interacting ozone and CO₂ in *Populus tremuloides*. *Chemosphere* 36, 807–812.
- Karnosky, D.F., Mankovska, B., Percy, K., Dickson, R.E., Podila, G.K., Sober, J., Noormets, A., Hendry, G., Coleman, M.D., Kubiske, M., Pregitzer, K.S., Isebrands, J.G., 1999. Effects of tropospheric O₃ on trembling aspen and interaction with CO₂: results from an O₃-gradient and a FACE experiment. *Water, Air and Soil Pollution* 116, 311–322.
- Kirschbaum, M.U.F., 2000. Forest growth and species distribution in a changing climate. *Tree Physiology* 20, 309–322.
- Kolb, T.E., Fredericksen, T.S., Steiner, K.C., Skelly, J.M., 1997. Issues in scaling tree size and age responses to ozone: a review. *Environmental Pollution* 98, 195–208.
- Krupa, S.V., Manning, W.J., 1988. Atmospheric ozone: formation and effects on vegetation. *Environmental Pollution* 50, 101–137.
- Kull, O., Sober, A., Coleman, M.D., Dickson, R.E., Isebrands, J.G., Gagnon, Z., Karnosky, D.F., 1996. Photosynthetic responses of aspen clones to simultaneous exposures of ozone and CO₂. *Canadian Journal of Forestry Research* 26, 639–648.
- Laisk, A., Kull, O., Moldau, H., 1989. Ozone concentration in leaf intercellular air spaces is close to zero. *Plant Physiology* 90, 1163–1167.

- Larson, P.R., 1977. Phyllotactic transitions in the vascular system of *Populus deltoides* bartr. As determined by ^{14}C labelling. *Planta* 134, 241–249.
- Larson, P.R., Isebrands, J.G., 1971. The plastochron index as applied to developmental studies of cottonwood. *Canadian Journal of Forest Research* 1, 1–11.
- Long, S.P., 1991. Modification of the response of photosynthetic productivity to rising temperature by atmospheric CO_2 concentrations: has its importance been underestimated? *Plant, Cell and Environment* 14, 729–739.
- Long, S.P., 1994. Increases in temperature, CO_2 and O_3 on net photosynthesis, as mediated by Rubisco. In: Alscher, R.G., Wellburn, A.R. (Eds.), *Plant Responses to the Gaseous Environment: Molecular, Metabolic and Physiological Aspects*. Chapman and Hall, London, pp. 21–38.
- McLaughlin, S., Percy, K., 1999. Forest health in North America: some perspectives on actual and potential roles of climate and air pollution. *Water, Air and Soil Pollution* 116, 151–197.
- McKee, I.F., Farage, P.K., Long, S.P., 1995. The interactive effects of elevated CO_2 and O_3 on photosynthesis in spring wheat. *Photosynthesis Research* 45, 111–119.
- Martin, M.J., Farage, P.K., Humphries, S.W., Long, S.P., 2000. Can the stomatal changes caused by acute ozone exposure be predicted by changes occurring in the mesophyll? A simplification for models of vegetation response to the global increase in tropospheric elevated ozone episodes. *Australian Journal of Plant Physiology* 27, 211–219.
- Melillo, J.M., Prentice, I.C., Farquhar, G.D., Schulze, E.-D., Sala, O.E., 1996. Terrestrial biotic responses to environmental change and feedbacks to climate. In: Houghton, J.T., Meira Filho, L.G., Callander, B.A., Harris, N., Kattenberg, A., Maskell, K. (Eds.), *IPCC: Climate Change 1995*. Cambridge University Press, Cambridge, pp. 445–481.
- Norby, R.J., Wullschlegel, S.D., Gunderson, C.A., Johnson, D.W., Ceulemans, R., 1999. Tree responses to rising CO_2 in field experiments: implications for the future forest. *Plant, Cell and Environment* 22, 683–714.
- Pell, E.J., Eckhart, N.A., Glick, R.E., 1994. Biochemical and molecular basis for impairment of photosynthetic potential. *Photosynthesis Research* 39, 453–462.
- Pell, E.J., Sinn, J.P., Brendley, B.W., Samuelson, L., Vinten-Johansen, C., Tien, M., Skillman, J., 1999. Differential response of four tree species to ozone-induced acceleration of foliar senescence. *Plant, Cell and Environment* 22, 779–790.
- PORG, 1993. Ozone in the United Kingdom. In: Third Report of the United Kingdom Photochemical Oxidants Review Group. AEA Harwell Laboratory, Didcot, UK, pp. 59–66.
- Rauscher, H.M., Isebrands, J.G., Host, G.E., Dickson, R.E., Dickmann, D.I., Crow, T.R., Michael, D.A., 1990. ECOPHYS: an ecophysiological growth process model for juvenile poplar. *Tree Physiology* 7, 255–281.
- Reynolds, J.F., Hilbert, D.W., Kemp, P.R., 1993. Scaling ecophysiology from the plant to the ecosystem: a conceptual framework. In: Ehleringer, J.R., Field, C.B. (Eds.), *Scaling Physiological Processes: Leaf to Globe*. Academic Press, San Diego, pp. 127–140.
- Schmieden, U., Wild, A., 1995. The contribution of ozone to forest decline. *Physiologia Plantarum* 94, 371–378.
- Sharkey, T.D., 1985. O_2 -insensitive photosynthesis in C_3 plants. *Plant Physiology* 78, 71–75.
- Stitt, M., Krapp, A., 1999. The interaction between elevated carbon dioxide and nitrogen nutrition: the physiological and molecular background. *Plant, Cell and Environment* 22, 583–621.
- Theseira, G., Host, G.E., Isebrands, J.G., Whisler, F.D., 2001. SOILPSI: a potential-driven three-dimensional soil water redistribution model: description and comparative evaluation. *Environmental Modeling and Software*, submitted for publication.
- von Caemmerer, S., Farquhar, G.D., 1981. Some relationships between the biochemistry of photosynthesis and the gas exchange of leaves. *Planta* 153, 376–387.
- Wu, G. 1999. A parallel implementation of numerical experiments investigating the shading characteristics of *Populus Eugeneii*. Master's thesis in Applied and Computational Mathematics, University of Minnesota–Duluth.
- Yun, S.-C., Laurence, J.A., 1999. The response of clones of *Populus tremuloides* differing in sensitivity to ozone in the field. *New Phytologist* 141, 411–421.
- Zang, G., 1999. Development of regulatory components for ECO-PHYS. Master's thesis in Applied and Computational Mathematics, University of Minnesota–Duluth.
- Zhao, W., 2000a. Technical Report 2000-3. University of Minnesota–Duluth.
- Zhao, W., 2000b. An analytical solution for a mechanistic photosynthesis model. Master's thesis in Applied and Computational Mathematics, University of Minnesota–Duluth.